Electrical tip-sample contact in scanning conductive torsion mode

Stefan A. L. Weber and Rüdiger Berger

Citation: Appl. Phys. Lett. **102**, 163105 (2013); doi: 10.1063/1.4802725
View online: http://dx.doi.org/10.1063/1.4802725
View Table of Contents: http://apl.aip.org/resource/1/APPLAB/v102/i16
Published by the American Institute of Physics.

Electrical tip-sample contact in scanning conductive torsion mode

Stefan A. L. Weber[a)] and Rüdiger Berger
Max Planck Institute for Polymer Research, Ackermannweg 10, 55128 Mainz, Germany

(Received 28 February 2013; accepted 4 April 2013; published online 23 April 2013)

We investigated the nature of the mechanical and the electrical tip-sample contact in scanning conductive torsion mode microscopy (SCTMM). Experiments on the soft conducting polymer blend of poly(3,4-ethylenedioxythiophene) poly(styrenesulfonate) demonstrated that the tip-sample force and thus the danger of tip-induced sample damage can be minimized. Using current-voltage spectroscopy, we found a space-charge limited conduction behavior with no indication of a tunneling barrier. Spectroscopy and imaging experiments showed that SCTMM allows for a gentler tip-sample contact compared to conventional conductive scanning force microscopy. A gentle and well-defined contact is a prerequisite for reproducible scanning probe based conductivity measurements, in particular on soft organic materials. © *2013 AIP Publishing LLC* [http://dx.doi.org/10.1063/1.4802725]

For the development and fabrication of flexible electronic devices, organic electronic materials become more and more important. This class of functional materials demands specialized methods for local electrical characterization on a nanometer scale. Here, scanning probe microscopy is the method of choice, as it allows for gentle topographic imaging in combination with electrical characterization.[1,2] In particular, conductive scanning force microscopy (C-SFM) has been widely used for mapping sample conductance[3–7] and photo currents.[8,9] However, a limitation in the characterization of soft, fragile structures is given by the operation of C-SFM in contact mode. Hereby, high lateral forces can be exerted on the sample by the scanning tip, leading to wear of the sample surface.[10] In particular, soft organic electronic materials suffer from tip induced wear effects.[4,11]

Recently, the electrical tip-sample current was measured upon controlling the maximum force ("peak force") in a series of fast force distance curves.[12] Here, the tip-sample distance is modulated periodically. During the contact time of the tip with the sample surface, the current flow is measured. This method was used to map surface morphology of semiconductor polymer–carbon nanotube hybrid materials. The authors reported that no sample wear effects caused by the imaging process could be observed. However, the current has to be measured during the contact time between tip and sample surface. During the contact, the tip sample loading force and thus the tip sample contact area change continuously. These changes lead to variations in contact resistance and thus to changes in current flow. In order to completely track this dynamic process, the current detection has to happen at a high detection bandwidth and local IV spectroscopy becomes practically impossible under imaging conditions.

Alternatively, the tip-sample current can be measured continuously by using scanning conductive torsion mode microscopy (SCTMM).[1,13,14] This dynamic mode allows keeping a constant force between tip and sample without the above mentioned restriction in terms of current detection bandwidth. SCTMM was used to map the electrical current flow within fragile three dimensional structures such as polymeric nano-pillars.[13] In torsion mode, the base of a rectangular cantilever is vibrated by a pair of piezoelectric actuators that are driven antiperiodically[15] (Figure 1) and a torsional resonance mode can be excited in the cantilever. Similar to the conventionally used intermittent contact mode, the torsional vibration amplitude is reduced when the tip approaches the sample surface. This damping is caused by tip-sample interactions such as surface forces and in-plane interactions such as friction.[16] The decrease in amplitude is used as a feedback signal for the tip-sample separation.

During imaging, the tip oscillates in close proximity to the sample. Although some groups speak of a torsion mode as a "non-contact" technique,[14] it is very likely that the tip is in physical contact with the sample during imaging. Yurtsever *et al.* concluded from frequency modulation experiments on a block-copolymer sample that the tip actually oscillates "within the first motile top layer of the polymer surface" even at moderate setpoints.[17] In a previous work, we demonstrated that with decreasing torsional amplitude setpoint, the average tip-sample current increased.[13] From the observed current images, we concluded that with decreasing setpoint deeper regions of the sample can be probed. This observation indicates that stronger mechanical interaction also leads to improved charge transfer between tip and sample. One possible explanation for this behavior is to assume a tunnel contact between tip and sample. In this scenario, a decreased setpoint would result in a reduction of the tunnel barrier and thus in larger tip-sample current. Fowler-Nordheim tunneling is commonly used to describe the contact between a metallic tip and an inorganic semiconductor.[18] On organic semiconductors, however, the tip-sample contact resistance usually plays a minor role and the current is limited by the transport properties of the organic film. Most commonly, the currents can be explained by a space charge limited current behavior.[19–22] For an organic semiconductor film sandwiched between two ohmic contacts with the same lateral dimensions as the polymer film, the so-called Mott-Gurney law[19] predicts a current density j of

[a)]Author to whom correspondence should be addressed. Electronic mail: Stefan.Weber@mpip-mainz.mpg.de

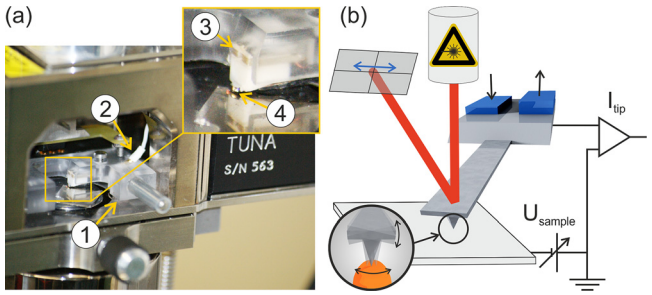

FIG. 1. (a) Torsion mode experiment in our Lab. Cantilever holder (1) with an electrical connection to a current amplifier (2). The split piezo (3) can drive the chip and the cantilever (4) to exert a periodic torsional momentum to the cantilever. (b) Schematic of the SCTMM working principle. A pair of antiperiodically driven piezoactuators (blue) excites a torsional vibration in the cantilever. Upon applying a voltage U_{sample} between tip and sample a current I_{tip} can be measured with a current amplifier.

$$j = \frac{9}{8}\,\mu\varepsilon_0\varepsilon\frac{U^2}{d^3}, \tag{1}$$

where μ is the charge carrier mobility, ε_0 and ε are the vacuum and relative dielectric permittivity, U is the voltage, and d is the distance between the electrodes.

In this work, we performed distance and bias spectroscopy experiments as well as comparative contact and torsion mode imaging in order to elucidate the physical nature of the mechanical and the electrical contact, respectively. As model sample we used a standard conducting polymer blend made of poly(3,4-ethylenedioxythiophene) poly(styrenesulfonate) (PEDOT:PSS). PEDOT:PSS thin films are often used in organic electronic devices and have been subject to a number of studies using conventional C-SFM.[4,5,22,23] We prepared films of PEDOT:PSS (Sigma Aldrich, high-conductivity grade, CAS: 155090-83-8) by spin-coating on a Pt coated silicon wafer. After the deposition, the films were annealed in a vacuum oven for 45 min at 140 °C.

The experiments have been performed on a Veeco Multi Mode (NanoScope V Controller) with NanoSensors PPP-EFM cantilevers with a Pt/Ir coating. The vertical force constant was determined to be 2.2 N/m with the thermal noise method.[24] The lateral deflection sensitivity was determined to be $(37.6 \pm 0.2)\,\mathrm{nm\,V^{-1}}$ for cantilevers with a tip cone height of 15 μm. The torsional resonance frequency was determined to be 892 kHz. At this frequency and at a torsional amplitude of 10 nm, no vertical motion was measured. A tune graph and the details of the calibration are given in the supplementary material.[25]

In a first experiment, we studied the torsional amplitude and the vertical cantilever deflection while approaching and retracting the tip towards the sample surface of the PEDOT:PSS film (Figure 2). During the approach, we observed a discontinuous jump (snap-in) in both amplitude and deflection (blue curves in Figures 2(a) and 2(b)). The amplitude dropped by a factor of one third, from 9.8 nm to 6.7 nm. Simultaneously, the normal force jumped to a value of −4.8 nN. During the further approach, the torsion amplitude decreased monotonically, whereas the vertical cantilever force remained stable around −5.2 nN. Finally, in a second snap-in, the tip established a stable contact with the surface. Now, the amplitude had a constant value of (620 ± 20) pm and the force

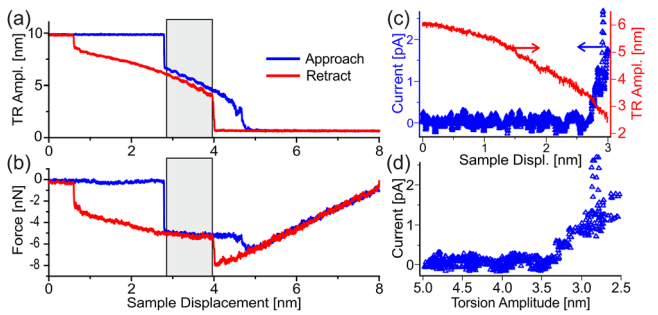

FIG. 2. Distance spectroscopy experiments. Simultaneously recorded torsion amplitude (a) and vertical force (b). The torsion amplitude (red line) and the tip-sample current (blue triangles) are shown as a function of sample displacement (c) and the same data replotted as current vs. torsion amplitude (d).

increased linearly. In the retract curve, both jump events can be observed again with a hysteresis of a few nanometers. This hysteretic behaviour has been observed before for torsional distance spectroscopy.[15]

The operation range for torsion mode imaging is marked with a grey box in Figures 2(a) and 2(b). The torsion amplitude decreased monotonically with tip-sample distance within that range, providing a useful feedback signal for the height control loop. The upper operation limit is given by the first snap-in event, where the cantilever was bent downwards due to attractive forces acting between tip and sample. In spite of the mechanical contact with the sample, the tip was able to move laterally while in-plane friction forces lead to a damping of the torsional vibration. This damping increased while the sample was further approached until it finally dropped to a value close to zero. The reason for the non-zero oscillation amplitude is probably a residual torsional motion of the cantilever due to the excitation. This second jump-in marks the lower operation limit for torsion mode imaging.

Please note that throughout the stable operation regime, the cantilever was bending downwards. In contact mode, stable operation is possible only at positive cantilever deflection as the deflection signal is used for the feedback. Furthermore, the negative cantilever deflection suggests that the tip is in permanent contact with the sample owing to attractive tip-sample forces. The clear first snap-in measured in the torsion mode amplitude suggests that an intermittent contact is unlikely.

Due to the permanent proximity of tip and sample, charge carriers can be exchanged between the tip and a conductive sample at sufficiently high voltage differences. This was demonstrated in an additional distance spectroscopy experiment, where a tip-sample bias of 3.2 V was applied (Figures 2(c) and 2(d)). The z-approach was stopped by a trigger before the second snap-in to prevent destructively high currents exceeding the measurement range of the current amplifier. We observed such high currents in the contact regime already at very moderate sample voltages of 12 mV (see supplementary material[25]). On the last nanometer of the approach, a fast increase of the current to up to 2.5 pA was observed. The strong distance dependence of the current signal demonstrates that the choice of imaging parameters such as amplitude setpoint and sample bias is crucial for current imaging. This delicate relationship is demonstrated by plotting the tip-sample current versus the torsional amplitude

(Fig. 2(d)). A significant tip-sample current could only be measured at amplitudes lower than 3.5 nm or 35% of the free vibrating amplitude. We will demonstrate below that the local current is also strongly influenced by the sample heterogeneity.

To further investigate the electrical properties of this contact, we performed bias spectroscopy experiments where we recorded the tip-sample current while ramping the sample bias from 0 V to 9 V (Figure 3(a)). During this experiment, the tip was engaged to the sample in torsion mode at an amplitude setpoint of 5 nm (50% of the free amplitude). Below a sample voltage of 2 V, the current amplifier recorded only noise (noise level $\sim$ 50 fA). Between 3 V and 8 V, the current increased to 10 pA, the higher limit of the amplifier's measurement range. Close to 9 V, the current signal became unstable, suggesting the onset of irreversible processes in the PEDOT:PSS film. Such effects have been observed before in contact mode C-SFM experiments at much lower tip-sample voltages of around 5 V.[4]

The linear appearance of the curve in the double-logarithmic plot over a wide voltage range suggests a power law dependence of the current on the sample bias in correspondence to a space-charge limited conduction behavior (see Eq. (1)). Fitting the data with a power law yielded an exponent of 3.788 ± 0.004. This is almost twice compared to the expected exponent of 2.

Deviations from the ideal space charge limited behavior have been reported on organic semiconductors before and are usually explained by an electric field dependent charge carrier mobility, e.g., by a Poole-Frenkel type behavior[22,23,26]

$$\mu = \mu_0 \exp\left(\sqrt{E/E_0}\right). \tag{2}$$

Here, μ_0 is the zero field mobility, $E = U/L$ is the electric field, and E_0 is the field coefficient.

The voltage dependent charge carrier mobility can be calculated by rearranging Eq. (1)

$$\mu(U) = \frac{8L^3 I}{9\,\varepsilon_0 \varepsilon\, U^2 A}, \tag{3}$$

where L is the film thickness and A is the contact area between tip and sample. In Figure 3(b), the charge carrier mobility as calculated from Eq. (3) is displayed together with a Poole-Frenkel fit according to Eq. (2). The zero-field mobility obtained from the fit in Figure 3(b) yielded a value of $(6.56 \pm 0.16) \times 10^{-5}$ cm^2/V s. This value is significantly lower compared to values reported for C-SFM bias spectroscopy on PEDOT:PSS before.[23]

For a more exact calculation of the mobility, it has to be taken into account that in an C-SFM experiment the assumption of large electrodes required for the derivation of Eq. (1) is no longer satisfied, as the tip forms a nanoscale contact with the sample. Reid *et al*. performed finite element simulations to study the current distribution through a thin film of an organic semiconductor.[20] They found a current distribution that extended laterally much wider than the contact area of the tip. This leads to deviations from the classical Mott-Gurney law. However, the modified space charge limited current model proposed by Reid *et al*. yields even lower mobility values compared to Eq. (3).

Further deviations can originate from variations in the tip-sample force due to the changing electrostatic forces during a voltage sweep. Variations in the vertical force, however, have an impact on the tip-sample friction and thus on the torsional vibration amplitude. In order to test if the height feedback will compensate for this additional force, we recorded the vertical deflection during a voltage sweep experiment (supplementary material[25]). At both positive and negative voltages, the cantilever was bent downwards due to the feedback retracting the cantilever, keeping the effective tip-sample force constant. Please note that the effect of electrostatic fields is different in contact mode. Here, the feedback keeps the deflection constant. Thus, the effective tip-sample force will increase towards higher voltage values. So compared to contact mode, SCTMM is less prone to artifacts caused by electrostatic forces.

In heterogeneously conducting materials such as the PEDOT:PSS, the exact current distribution in the sample is determined by the three dimensional structure and thus by the conducting pathways through the sample.[23,27,28] It has been shown that humidity can lead to a selective swelling of the hydrophilic PSS domains and thus to a change in the electric properties.[29] Furthermore, it is known that PEDOT:PSS blends form an insulating PSS rich top layer. Kemerink *et al*. found a transition from a space charge limited to an ohmic behavior when they moved a tunneling microscopy tip into deeper regions in a PEDOT:PSS film.[22] They concluded that in the PEDOT rich bulk of the film the conductivity $\sigma = q\ n\ \mu$ (q: elementary charge, n: charge carrier density) was sufficiently high, leading to a reduction of space charge effects. Thanks to the significantly lower cantilever load force in SCTMM, the tip penetrates the insulating PSS-rich top layer much less compared to C-SFM in contact mode. Therefore, the tip-sample current is dominated by the electrical properties of this top layer, yielding comparably low mobility values. Finally, small variations in the tip-sample distance during one oscillation cycle, as discussed

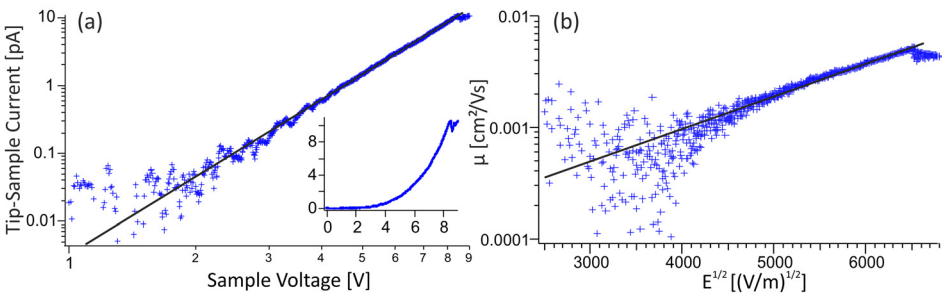

FIG. 3. SCTMM bias spectroscopy experiment. (a) current-voltage graph (inset: same data with linear axes). (b) Charge carrier mobility as a function of the square root of the electric field $E = U/L$ (film thickness $L = 200$ nm, contact radius $r = 5$ nm, dielectric constant $\varepsilon = 3$). The straight line is a Poole-Frenkel fit yielding a zero field charge carrier mobility of $(6.56 \pm 0.16) \times 10^{-5}$ cm^2/Vs.

in an earlier paragraph, could lead to an effective deterioration of the electrical contact.

In order to demonstrate the imaging capabilities of SCTMM, topography images (Figures 4(a) and 4(b)) were recorded simultaneously with current maps ((c) and (d)). The sample bias was 7 V and the torsional amplitude setpoint 5.2 nm (73% of the free amplitude). In order to assess possible irreversible alterations in the sample structure and conductivity, we first imaged a $(1 \times 1)\ \mu m^2$ area ((a) and (c)) and subsequently increased the scan area to $(3 \times 3)\ \mu m^2$ ((b) and (d)). The previously scanned area is marked by a white dashed box in (b) and (d). The topography shows a granular structure with a root-mean-square (RMS) roughness of 7.9 nm in the small scale image (a). The topography in the previously scanned area in the larger scale image (b) was almost unchanged with a RMS roughness of 8.2 nm (8.9 nm for the entire image). Most significantly, no pileup of material could be found on either side of the previously scanned area in (b). In contact mode experiments on soft surfaces, this is a common feature that is observed when the tip is scratching the surface.[30]

On the current imaging channel, we found some 100 nm large areas with homogeneous currents of up to 6 pA. The streaky horizontal features were most likely caused by slight variations in the tip-sample contact between subsequent scanlines, e.g., due to tip contamination. Such features are hard to avoid in this current regime. Next to the larger scale structures, 30–40 nm wide worm-like current patterns can be found throughout the current images (arrows in Fig. 4(c)). Previous studies using C-SFM on PEDOT:PSS samples consistently reported strongly localized spots of high currents surrounded by a mostly insulating background.[4,5,31,32] Both the structure and the magnitude of the current remained stable in the subsequent large area scan in (d). The average current recorded in the first image was (1.3 ± 0.7) pA and it reduced slightly to (1.1 ± 0.6) pA in the same area of the subsequent image. The rest of the image (area outside the box in (d)) carried a current of (1.2 ± 0.6) pA, indicating a

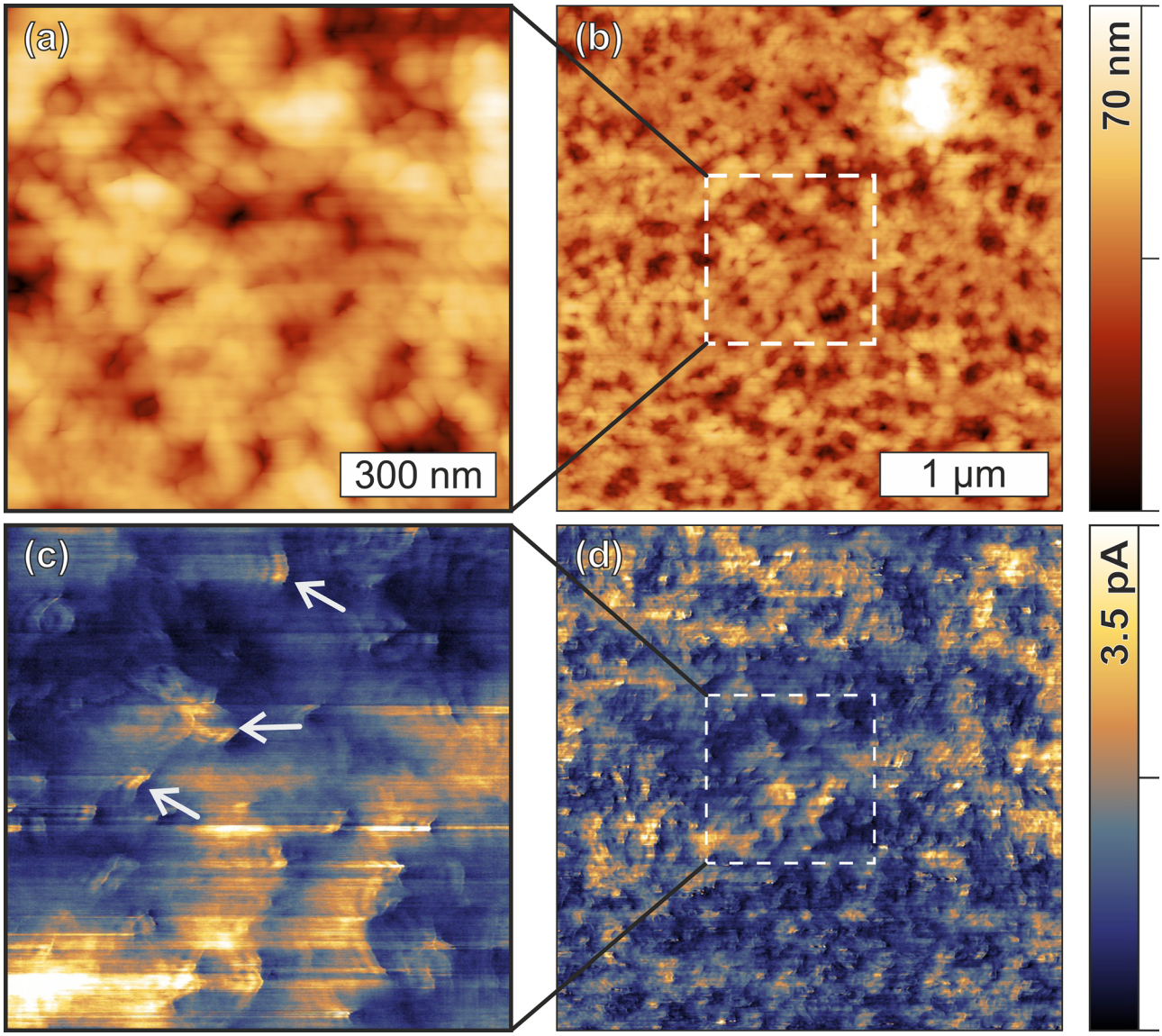

FIG. 4. SCTMM Images of the PEDOT:PSS surface topography ((a) and (b)) and simultaneously recorded tip-sample current at a sample bias of 7 V ((c) and (d)). The $(1 \times 1)\ \mu m^2$ images on the left hand side ((a) and (c)) were recorded first. Afterwards, the scan size was increased to 3 μm. The previously scanned area is marked with the white dashed box in (b) and (d). In the current images, worm-like patterns (gray arrows) can be observed.

slight reduction in the sample conductivity. Such a C-SFM induced decrease of sample conductivity on PEDOT:PSS samples has been reported before. Dang *et al.* reported a complete transition to insulating behavior upon scanning the sample at a sample bias of more than 5 V.[4] This irreversible effect was accompanied by strong topographical changes, indicating a rearrangement of the constituents in the PEDOT:PSS inside the blend film. In our experiments, we never observed scanning induced topographical effects at tip-sample voltages of up to 9 V. This indicates that the mechanical interaction between tip and sample plays an important role for these previously reported irreversible effects.

In order to test if the significantly different current patterns observed by SCTMM were caused by the sample or by the imaging method, we changed the imaging mode to conventional contact mode C-SFM using the same tip and sample at a much lower sample bias of 100 mV. The resulting images showed a blurred topography together with strongly localized current spots of up to 100 pA that were consistent to C-SFM images of PEDOT:PSS samples from the literature[4,5] (supplementary material[25]). These structures are most probably caused by the penetration of the PSS rich insulating top layer by the scanning tip. In contrast, the SCTMM current map showed a more homogeneous current pattern, indicating that the tip stays on top of the PSS top layer. This result again underpins the importance of a precise control of the tip-sample contact for C-SFM imaging experiments on soft organic materials.

In conclusion we have investigated the physics of the tip sample contact during SCTMM operation on the soft organic electronic material of PEDOT:PSS. The distance spectroscopy experiments have revealed that stable imaging is possible even at negative cantilever load force. The *effective* normal force acting on the sample during imaging is given by the sum of the cantilever load force, the tip-sample adhesion and electrostatic forces (see supplementary material[25]). Thus, the minimum effective imaging force for both contact mode and CSFS-AFM or "peak-force"[12] imaging would be the adhesion force plus the required positive cantilever deflection force. Operating in torsion mode, the effective tip-sample force can be better controlled and further minimized. In particular, for soft polymeric materials often found in organic electronics that is a decisive advantage as it further prevents tip induced sample damage.

Furthermore, SCTMM current-voltage spectroscopy showed a power law dependence of the current on the sample bias in correspondence to a space-charge limited conduction behavior. The measured charge carrier mobility and the SCTMM current maps indicate that the tip-sample currents were dominated by the electrically less conductive PSS-rich surface layer. Our results demonstrate that on soft organic materials having a gentle tip-sample contact is of utmost importance for a reliable interpretation of SPM data.

The support by the DFG IRTG program 1404 "Self-organized Materials for Optoelectronics" is gratefully acknowledged.

[1]R. Berger, H. J. Butt, M. B. Retschke, and S. A. L. Weber, Macromol. Rapid Commun. **30**(14), 1167 (2009).
[2]S. A. L. Weber, H. J. Butt, and R. Berger, in *Scanning Probe Microscopy in Nanoscience and Nanotechnology*, edited by B. Bhushan (Springer, Berlin, 2013), Vol. 3, p. 551.
[3]M. J. Loiacono, E. L. Granstrom, and C. D. Frisbie, J. Phys. Chem. B **102**(10), 1679 (1998).
[4]X. D. Dang, M. Dante, and T. Q. Nguyen, Appl. Phys. Lett. **93**(24), 241911 (2008).
[5]L. S. C. Pingree, B. A. MacLeod, and D. S. Ginger, J. Phys. Chem. C **112**(21), 7922 (2008).
[6]S. A. L. Weber, M. Memesa, R. Berger, H. J. Butt, and J. S. Gutmann, J. Nanosci. Nanotechnol. **10**, 6840 (2010).
[7]M. Memesa, S. A. L. Weber, S. Lenz, J. Perlich, R. Berger, P. Muller-Buschbaum, and J. S. Gutmann, Energy Environ. Sci. **2**(7), 783 (2009).
[8]D. C. Coffey, O. G. Reid, D. B. Rodovsky, G. P. Bartholomew, and D. S. Ginger, Nano Lett. **7**(3), 738 (2007).
[9]L. S. C. Pingree, O. G. Reid, and D. S. Ginger, Nano Lett. **9**(8), 2946 (2009).
[10]A. Dasari, Z. Z. Yu, and Y. W. Mai, Mater. Sci. Eng., R **63**(2), 31 (2009).
[11]O. Douheret, A. Swinnen, M. Breselge, I. Van Severen, L. Lutsen, D. Vanderzande, and J. Manca, Microelectron. Eng. **84**(3), 431 (2007).
[12]S. Desbief, N. Hergue, O. Douheret, M. Surin, P. Dubois, Y. Geerts, R. Lazzaroni, and P. Leclere, Nanoscale **4**, 2705 (2012).
[13]S. A. L. Weber, N. Haberkorn, P. Theato, and R. Berger, Nano Lett. **10**(4), 1194 (2010).
[14]A. Vetushka, T. Itoh, Y. Nakanishi, A. Fejfar, S. Nonomura, M. Ledinský, and J. Kočka, J. Non-Cryst. Solids **358**(17), 2545 (2012).
[15]L. Huang and C. Su, Ultramicroscopy **100**(3–4), 277 (2004).
[16]T. Kawagishi, A. Kato, Y. Hoshi, and H. Kawakatsu, Ultramicroscopy **91**(1–4), 37 (2002).
[17]A. Yurtsever, A. M. Gigler, C. Dietz, and R. W. Stark, Appl. Phys. Lett. **92**(14), 143103 (2008).
[18]A. Olbrich, B. Ebersberger, and C. Boit, Appl. Phys. Lett. **73**(21), 3114 (1998).
[19]N. F. Mott and R. W. Gurney, *Electronic Processes in Ionic Crystals*, 2nd ed. (Oxford University Press, London, 1950).
[20]O. G. Reid, K. Munechika, and D. S. Ginger, Nano Lett. **8**(6), 1602 (2008).
[21]H. N. Lin, H. L. Lin, S. S. Wang, L. S. Yu, G. Y. Perng, S. A. Chen, and S. H. Chen, Appl. Phys. Lett. **81**(14), 2572 (2002).
[22]M. Kemerink, S. Timpanaro, M. M. de Kok, E. A. Meulenkamp, and F. J. Touwslager, J. Phys. Chem. B **108**(49), 18820 (2004).
[23]C. Ionescu-Zanetti, A. Mechler, S. A. Carter, and R. Lal, Adv. Mater. **16**(5), 385 (2004).
[24]J. E. Sader, J. W. M. Chon, and P. Mulvaney, Rev. Sci. Instrum. **70**(10), 3967 (1999).
[25]See supplementary material at http://dx.doi.org/10.1063/1.4802725 for supplemental figures and the calibration procedure.
[26]P. N. Murgatroyd, J. Phys. D: Appl. Phys. **3**(2), 151 (1970).
[27]S. Timpanaro, M. Kemerink, F. J. Touwslager, M. M. De Kok, and S. Schrader, Chem. Phys. Lett. **394**(4–6), 339 (2004).
[28]A. M. Nardes, M. Kemerink, R. A. J. Janssen, J. A. M. Bastiaansen, N. M. M. Kiggen, B. M. W. Langeveld, A. J. J. M. van Breemen, and M. M. de Kok, Adv. Mater. **19**(9), 1196 (2007).
[29]S. Magonov, Int. J. Polym. Anal. Charact. **16**(8), 505 (2011).
[30]S. A. Pihan, S. G. J. Emmerling, H.-J. Butt, J. S. Gutmann, and R. Berger, Wear **271**(11–12), 2852 (2011).
[31]H. Yan and H. Okuzaki, Synth. Met. **159**(21–22), 2225 (2009).
[32]H. J. Lee, J. Lee, and S.-M. Park, J. Phys. Chem. B **114**(8), 2660 (2010).